Vertical distribution of aerosols over the Maritime Continent during El Nino

Jason Blake Cohen[1], Daniel Hui Loong Ng[2], Alan Wei Lun Lim[3], Xin Rong Chua[4]

[1]School of Atmospheric Sciences, Sun Yat-Sen University, Guangzhou, China
[2]Tropical Marine Science Institute, National University of Singapore, Singapore
[3]The Chinese University of Hong Kong, Hong Kong, China
[4]Princeton University, Princeton, NJ, USA

Correspondence to: Jason Blake Cohen (jasonbc@alum.mit.edu)

Abstract. The vertical distribution of aerosols over Southeast Asia, a critical factor of aerosol lifetime, and impact on radiative forcing and precipitation, is examined for the 2006 post El-Nino fire burning season. Additionally, through analysis of measurements and modeling, we have reconfirmed the hypothesis that fire radiative power is underestimated. Our results are significantly different from what others are using. The horizontally constrained Maritime Continent's fire plume median height, using the maximum variance of satellite observed Aerosol Optical Depth as the spatial and temporal constraint, is found to be 2.17 ± 1.53km during the 2006 El Nino season. This is 0.96km higher than random sampling and all other past studies, with 62% of particles in the free troposphere. The impact is that the aerosol lifetime will be considerably longer, and that the aerosols will disperse in a direction different from if they were in the boundary layer. Application of a simple plume rise model using measurements of fire properties underestimates the median plume height by 0.34km and more in the bottom-half of the plume. The center of the plume can be reproduced when fire radiative power is increased by 20% (range from 0% to 100%). However, to reduce the biases found, improvements are required in terms of measurements of fire properties when cloud covered, representation of small scale convection, and inclusion of aerosol direct and semi-direct effects. The results provide the unique aerosol signature of fire under El-Nino conditions.

Deleted: significantly

1. Introduction

Properly quantifying the vertical distribution of aerosols is essential to constrain their atmospheric distribution, and in turn, the atmospheric energy budget [*Ming et al.*, 2010; *Kim et al.*, 2008], and understand their impact on circulation, clouds and precipitation [*Tao et al.*, 2012; *Wang* 2013], and human health [*Burnett et al*, 2014]. However, there are complicating factors including spatial and temporal heterogeneity in emissions [*Cohen and Wang*, 2014; *Cohen*, 2014; *Giglio et al.*, 2006; *Petrenko et al.*, 2012; *Wooster et al.*, 2012], and uncertainties and non-linearities associated with aerosol processing and removal from the atmosphere [Tao et al., 2012; *Cohen* and *Prinn*, 2011; *Cohen et al.*, 2011]. Furthermore, a lack of sufficiently dense measurements leads to difficulty constraining the measured distribution of aerosols over scales from hundreds to thousands of kilometers or over time frames on the decadal to longer time scales [Cohen and Wang, 2014; *Delene* and *Ogren*, 2002; *Dubovik et al.*, 2000; *Cohen* et al., 2017].

Models are very poor at reproducing the actual vertical distribution of atmospheric aerosols [*Cheng et al.*, 2012; *Schuster et al.*, 2005; *Tsigaridis et al.*, 2014]. They also tend to strongly underestimate the total atmospheric column loading of aerosols [*Colarco et al.*, 2004; *Leung et al.*, 2007]. Furthermore, vertical measurements are sparse, and in many regions do not provide adequate statistics to make informed comparisons with real world conditions. This is no more apparent than over Southeast Asia, where model studies [*Tosca et al.*, 2011; *Martin et al.*, 2012] have concluded that almost all aerosols are narrowly confined in the planetary boundary layer, although measurements demonstrate otherwise [*Lin et al.*, 2014]. Presently, there are no known modeling efforts that have been able to reproduce this significant atmospheric loading and the ensuing vertical distribution.

Additionally, aerosol emissions databases in Southeast Asia are quantified using a bottom-up approach, where small samples and statistics of the activity, land-use, economics, population, and hotspots are aggregated [*van der Werf*, 2010; *Lamarque*, 2010; *Bond et al.*, 2004]. This generally leads to sizable bias, since there are few measurements and rapidly changing land-surface features over Southeast Asia. A recent couple of papers, using measurements and models in tandem, has quantified a significant underestimation in aerosol emissions over Southeast Asia in terms of magnitude [*Cohen and Wang*, 2014], spatial, and temporal distribution [*Cohen*, 2014], including interannual and intraannual variation from fires.

Furthermore, the vertical distribution is uncertain due to incomplete understanding of in-situ production and removal mechanisms, which are dependent on washout, which is also poorly modeled [*Tao et al.*, 2012; *Wang* 2013], especially in the tropics during the dry season [*Petersen and Rutledge*, 2001; *Ekman et al.*, 2012], due to the random nature of convective precipitation. Heterogeneous aerosol processing may also change the hygroscopicity and hence vertical distribution of the aerosols [*Kim et al.*, 2008; *Cohen et al.*, 2011]. These factors have been show to combine such that small changes in the initial vertical distribution can lead to ultimate transport thousands of kilometers apart [*Wang,* 2013].

The Maritime Continent of Southeast Asia has faced widespread and ubiquitous fires the past few decades, due to expanding agriculture, urban development, economic growth, and changes in the base climatology that induce drought [*Center*, 2005; *Dennis et al.*, 2005; *van der Werf et al.*, 2008; *Taylor*,

Deleted: 6

Deleted: do a poor job of

Deleted: vertical distribution of

Deleted: as well as the related value of

Deleted: often

Deleted: providing

Deleted: the

Deleted: height is

Deleted: throughout the region

Deleted: .

Deleted: significant

Deleted: d

2010]. These fires contribute the major fraction of the atmospheric aerosol burden during the dry season [*Cohen*, 2014]. However, these fires are unique: they are relatively low in radiative power and temperature, yet cover a massive net surface area, making their statistics and extent hard to characterize from remote sensing. Yet, their total emissions are very high and they dominate the aerosol optical depth (AOD) and $PM_{2.5}$ levels over thousands of kilometers [*Field et al.*, 2009; *Nakajima et al.*, 1999]. Due to their widespread nature, fires in this region are geospatially coherent in their timing and geography, although individually they burn for different lengths of time, as a function of localized precipitation and soil moisture, and global circulation patterns such as El-Nino [*Cohen*, 2014; *Wooster et al.*, 2012; *Hansen*, 2008].

A comprehensive previous attempt to study aerosol height over Southeast Asia was performed by Lee et al. [2016]. They used the total CALIOP profile, but were not specific about how they cleared or accounted for high ice clouds that frequently found in this part of the world. Furthermore, they used satellite derived SSA to provide additional spatial resolution to go with each pass, but which has been shown to be highly error-prone over Southeast Asia [Rogers et al., 2009; Hostetler, 2008]. This work did not address how the spatially-disparate individual path measurements from CALIOP, sampling both fire plume and non fire plume pixels jointly, as compared to the approach used by Cohen [2014] and Cohen et al. [2017]. The few other attempts using CALIOP over this region have also been done, but without any local validation of the CALIOP product [Sugimoto et al., 2015], or have used models to validate the CALIOP measurements [Campbell et al., 2013].

Formatted: Font:

This work describes a new approach to comprehensively sample the vertical distribution of smoke aerosols, by first using decadal scale measurements of AOD from the MISR satellite [*Cohen*, 2014], and then separating the smoke impacted regions by the magnitude of the measured variability. During the 2006 El-Nino enhanced burning, one of the 2 largest such events over the past 15-year measurement record, this approach yields a much higher vertical aerosol height than the traditional random sampling approach. A simple plume-rise model [*Achtemeier et al.*, 2011; *Briggs*, 1965] using reanalysis meteorology [*Kalnay et al.*, 1996] and measured fire properties was found to underestimate the measured heights. However, the model could be improved to match the median heights by increasing the measured fire radiative power [*Sessions et al.*, 2011; *Sofiev et al.*, 2012], implying that the measured fires may be underestimated in terms of their strength, or that there are missing fires. However, the top and bottom heights of the measured plume still cannot be reproduced. The data shows that an improved representation of both localized convective transport and the aerosol direct and semi-direct effects [*Ekman et al.*, 2007; *Wang*, 2007] are required to make further improvements. It is hoped that these results will provide insight to those working on understanding the strong 2015-2016 El-Nino conditions.

2. Methods

2.1 Geography

This work is focused on the Maritime Continent, a sub region of Southeast Asia (8°S to 8°N, 95°E to 125°E) (**Figure 1**) that experiences wide-spread and highly emitting fires on a yearly basis during the

local dry season (August to October/November). The combined magnitude of the fires produces a single massive smoke plume, that covers much of the region, extending thousands of kilometers [*Cohen*, 2014]. These wide spread fires are due to anthropogenic clearing of rainforest and agriculture [*Cohen* et al., 2017; *Dennis et al.*, 2005; *van der Werf et al.*, 2008; *Taylor*, 2010; *Miettinen et al.*, 2013; *Langmann et al.*, 2009]. Over this region, during the dry season, the removal of aerosols is quite slow, leading to the overall properties of the plume being relatively consistent over space and time [*Cohen*, 2014]. Therefore, the overall properties of the smoke plume, when correctly bounded in space and time, can be robustly statistically related to the overall properties of individual fires, and daily measurements of AOD from the MISR satellite (**Figure 1**) [*Cohen*, 2014].

In 2006, the El-Nino conditions led to an enhanced drought, with subsequent fires lasting from September through November. To ensure that this event is uniquely and completely analyzed, only data from October is used. The region in (**Figure 1**) with the EOF (Bjornsson and Venegas, 1997; Cohen et al., 2017) of the measured MISR AOD larger than 2.2 is the net of the source regions (over land) and downwind regions (over both land and sea). This analytically provides a holistic representation in space and time of the impact of individual fires on the large-scale structure of the aerosol plume, hence allowing a comprehensive sampling of the vertical distribution of the smoke, including all sources, both observed and obscured by clouds (very common in this region), and aged aerosols downwind from their initial sources.

2.2 Measurements

CALIPSO is an active lidar that quantifies both the vertically resolved atmospheric backscatter strength (a reasonable approximation of the vertical profile of aerosols), and an indication of particle size (large or small) [*Winker et al.*, 2003]. Specifically, we use the backscatter at 532nm and the vertical feature mask (vertical resolution 30m, horizontal resolution 1/3km) [*Hostetler et al.*, 2006]. Since the width of each pass is narrow, they are not spatially representative in general. However, given the relative consistency of the plume as a whole, samples constrained within the plume's spatial extent, taken on the same day, are statistically representative of the smoke plume as a whole [*Cohen*, 2014].

The extinction-weighted top (10% vertically integrated height), middle-upper (30% vertically integrated height), median (50% vertically integrated height), middle-lower (70% vertically integrated height), and bottom (90% vertically integrated height) are computed for each individual measurement, with the values retained if the aerosol is not in the stratosphere (assumed to be 15km) **(Supplemental Figure 1)**. The data is then aggregated first by day, and secondly by geography, either into the fire-impacted region, or non fire-impacted region, based on (**Figure 1**) [*Cohen*, 2014]. The aggregated set of measurements is used to compute probability densities and statistics, demonstrating the vast difference over the fire-impacted and non-fire impacted regions (**Figures 2a,2b)**. with the vertical heights both significantly higher and less variable ($p<0.01$) over the fire region than the non-fire region.

Measurements of aerosol optical depth (AOD) [*Kaufman et al.*, 2003], fire radiative power (FRP) and fire temperature (T_F) [*Freeborn et al.*, 2014; *Ichoku et al.*, 2008] are obtained from the MODIS instrument aboard both the TERRA and AQUA satellites. Version 5, level 2, swath-by-swath measurements,

Deleted: 6

Deleted: the data analyzed is definitely from

Deleted: 6

Deleted: , thereby

Deleted: ing

Deleted: and

Deleted: s

Deleted: for

Deleted: observed fires, fires

Deleted: directly

Formatted: Font:Not Bold

at daily resolution are use for AOD (best solution 0.55 micron), with a spatial resolution of 10kmx10km, and FRP/T_F, with a spatial resolution of 1kmx1km. Given the prevalence of clouds in this region, the cloud-cleared products are used, leading to a possible low bias in the FRP/T_F measurements, as well as some fires not measured at all [*Cohen* et al., 2017; *Freeborn et al.*, 2014; *Ichoku et al.*, 2008; *Kahn et al.*, 2008; *Kahn et al.*, 2007]. On the other hand, while some grids are contaminated, the sheer spatial distance of the plume and the fact that the overwhelming majority of atmospheric aerosols during this time of the year are due to fires, means that there is no observable bias in the overall statistics of the measured AOD [*Cohen*, 2014], as observed by looking at the spatially averaged MODIS AOD and statistics over the fire-constrained and non fire-constrained regions (**Figure 3**). The AOD is higher ($p<0.01$) over the fire-constrained region, making the findings consistent with the approach employing the 12 years worth of MISR measurements.

In terms of MODIS retrieval uncertainties over land, especially during fire events, there are two important issues to consider. The first is that under extremely high AOD conditions (AOD>2), frequently aerosols are flagged/reclassified as clouds, which brings about a negative bias. This bias would lead to an even higher AOD over the fire plume region if it were properly handled, leading to an even larger difference between "fire region" and the "non-fire region". The second is the error in the over-land retrieval can go as high as 15%. However, based on the results in (**Figure 3 and Supplemental Figure 2**), the difference between the "fire region" and the "non-fire region" is statistically sound even assuming the error is larger than 15%. It is also the reason why MISR was used for the initial definition of the two regions, since its ability to cloud clear is better than MODIS over this region.

While there are are many errors involved with using the satellite data, the errors in this case are sufficiently small as to not impact the analysis and results over Southeast Asia during the fire season (Cohen, 2014; Cohen et al., 2017). The AOD and certain surface products, when used to run models, have been found to compare in magnitude, spatial, and temporal extent, to various ground based surface and column measurements, such as from AERONET, NOAA, and national pollution networks. The data-driven models have been shown to lead to a reduction in the annualized RMS error as compared with the IPCC RCP emissions scenarios by a factor of 2 to 8 against AERONET stations throughout Asia (Cohen and Wang, 2014). Furthermore, on a month-to-month basis, the results of the data-driven models have been shown to lead to a reduction in the RMS error by a factor of 1.8 and an improvement in the R2 statistic of 0.2 to 0.3 against the GDED Fire emissions dataset (Cohen 2014; Cohen et al. 2017). Given these findings, it is reasonable to assume that the methodology is as reliable as anything else presently available, with respect to this work.

2.3 Plume Rise Model

A simple model is employed to simulate the height to which a parcel of air initially at the surface over the fire will rise, based on buoyancy, vertical, and horizontal advection (**Supplement**). The formulation requires information about the temperature and radiative power of the fire as well as local meteorology [*Achtemeier et al.*, 2011; *Briggs*, 1965], and yields an idealized height to which aerosols

Deleted: 6

Deleted: significant

Deleted: significantly

Formatted: Font:Bold

emitted will rise. The buoyant plume rise is a thermodynamic approximation in nature and thus not as physically realistic as a large eddy approach, which solves the atmospheric fluid dynamical equations by parameterizing turbulence at the scale of tens of meters. However, it is less computationally expensive and more generalizable in the context of approximating the thousands of fires spread geographically over hundreds of thousands of square kilometers. On the other hand, it is more physically realistic than empirical relationships from multi-angle measurements [*Sofiev et al.*, 2012], which have also been attempted, but show poor performance in Southeast Asia.

These relationships are efficiently solved using measurements of meteorological and fire properties, allowing them to be used as rapid parameterizations within regional or global models. However, there are errors associated with reconciling the different temporal and spatial scales of reanalysis meteorology, especially convection and associated transport. Secondly, cloud-cover in this region leads to both missing fires and low-bias in measurements of fire properties [Sofiev et al., 2012; *Kaufman et al.*, 2003]. Third, the cloud-cover also leads to a heavier contribution of model results in the reanalysis meteorology. Finally, the effects of the optically thick aerosol plume's feedback on the radiative profile is likely important, but beyond the scope of this work and hence not taken into consideration [*Ekman et al.*, 2007; *Wang*, 2007].

Deleted:

Deleted: significant

3. Results and Discussion

3.1 Measured Aerosol Vertical Distribution

The fire-constrained monthly aggregated daily statistics of the measured vertical aerosol height from CALIPSO [*Winker et al.*, 2003] is given in (**Figure 2a**), with the monthly aggregated statistics over the fire-constrained region of the bottom, middle-lower, median, middle-upper, and top heights respectively: 1.68 ± 1.59km, 1.92 ± 1.55km, 2.17 ± 1.53km, 2.50 ± 1.54km, and 2.98 ± 1.55km (**Table 1**). On the other hand, the non fire-constrained region's monthly aggregated statistics of the measured vertical aerosol height is quite different (**Figure 2b**), with the respective bottom, middle-lower, median, middle-upper, and top heights: 0.65 ± 0.98km, 0.93 ± 0.98km, 1.21 ± 1.00km, 1.53 ± 1.02km, and 1.98 ± 1.08km (**Table 1**). The average aerosol height over the fire-constrained region is both much higher and more variable at every vertical level as compared to the non fire-constrained domain, with 62% of the aerosol loading in the free troposphere over the fire-constrained domain, while only 17% is located in the free troposphere over the non fire-constrained domain. However, the variability is roughly constant at all levels over the fire-constrained region, while the variability increases with vertical level, over the non fire-constrained region. These results are based on more than 10,000 daily CALIOP measurements.

All three findings, higher average aerosol height, larger variance of height, and a consistent variance of height at all levels, are consistent with areas where most of the aerosol loading is due to surface fires. Firstly, the buoyancy from fires increases the expected height, with differences in buoyancy from different strength fires producing random variability in the measured heights. So long as the distribution of fire strength and meteorology do not differ too much from day-to-day, the variance in aerosol heights should also not vary much. On the other hand, over non fire-constrained regions, the major contribution to

the vertical aerosol variability is convection, which is expected to increase in variability the higher one moves upwards from the surface.

Furthermore, the relatively constant variability across the heights in the fire-constrained region is consistent with a proposed radiative-stabilization effect. The extremely high measured AOD values found by MODIS [*Kaufman et al.*, 2003] over the fire-constrained domain (from 0.5 to 2.0, with most days over 1.0), leads to observable surface cooling (**Figure 3**). Additionally, BC emitted from the fire, absorbs incoming solar radiation near the upper portion of the plume, providing a source of warming. This combination leads to additional stabilization of the atmosphere, and therefore the vertical aerosol distribution.

Deleted: significant

Deleted: significant

These results are thus consistent with the observed reduction in in-situ vertical processing over the regions downwind from the fire sources, but still within the fire-constrained plume region, where buoyancy from the fires and the self-stabilization effect seem to contribute more than random deep convection. However, over the non fire-constrained region, given the low AOD and lack of fires, both of these effects are not observed, and convection dominates, which is consistent with the less uniform vertical distribution. Given these clear and observed differences, only results from the fire-constrained region will be considered further.

A significant amount of aerosol mass exists in the free troposphere over this region. By assuming that the measured boundary layer height of 1000m as observed in Singapore [*Chew et al.*, 2013] is applied to the domain, then 62%, 73%, 83%, 93%, and 98% of the total monthly respective measurements of the bottom, lower-middle, median, upper-middle and top extinction heights are located in the free troposphere. This is much higher than previous studies, which indicated most of the smoke remained within the boundary layer [*Tosca et al.*, 2011].

Analysis of the daily measured heights demonstrates 3 statistically unique days: October 11th, 15th and 22nd (**Table 2**). On the 11th, the top and upper-middle measurements fall within the top 15%, while the median measurements fall within the top 20% of the month's measurements, implying that the result is consistent with a deep, single layer, extending throughout the lower and middle free-troposphere. The 15th and 22nd, while not being as high in the middle-troposphere, also have little to no aerosol in the planetary boundary layer due to being more confined in the vertical, implying a narrow layer in the middle free-troposphere. These results are consistent with the measured aerosol layer being mostly in the free troposphere, a result that is not consistent with the measured FRP or meteorology, leading to two important implications. Firstly, the aerosol lifetime on these days will be considerably longer than models typically reproduce and the radiative forcing will be considerably more warming. Secondly, that typical modeling approach that fresh aerosols are mixed from the surface to the given top of the plume height is likely not true here, which has implications for the ability of most models to be able to correctly capture the aerosol loading.

Deleted: significantly

On the remaining days, the measured heights are consistent on a daily average basis with relatively uniform emissions, meteorology, and vertical buoyant rise. Although present, intense but heterogeneous

forcing impacting the vertical distribution, such as localized convection and aerosol cloud interactions are generally not observed to bias the overall plume's properties. Only on October 11th, 15th, and 22nd, are there higher heights or a narrower vertical structure, combined with no readily available explanation to be found in the fire, AOD, or meteorological properties on these days, indicating a likely clear change in the convection on those days, or some other phenomena not considered or captured by the reanalysis meteorology. The robustness of this approach assures the validity over the region and time period considered herein.

A comparison between the inverse model by Campbell et al. [2013; Supplemental Figure 6] and this work's underlying Kalman Filter plus variance maximization inversely modeled fields, shows that their model performs considerably less well during the biomass burning season, which is the focus of this work [Cohen, 2014; Cohen and Wang, 2014; Cohen et al., 2017]. Furthermore, the results found using the approach employed here, match well with individual measurement campaigns done by Lin Neng-Hui, et al. [2013, 2014, etc.], and the AD-Net measurement network [Sugimoto et al, 2014], that have focused on observations from a small number of on-the-ground lidar at multiple places within the Northern portion of Southeast Asia and Greater East Asia. While the geographic regions are not identical and therefore cannot be used to directly validate the region studied here, there is a sufficient amount of similarity, that there is some likelihood of overlap in the results. Given these factors, we present the results here as the best available for use at this time, when targeting this region of the world during the biomass burning season.

3.2 Measured Fire and Meteorological Properties

The daily aggregated measurements of fire radiative power (FRP) [*Freeborn et al.*, 2014; *Ichoku et al.*, 2008] indicate there are 109395 actively burning 1kmx1km pixels in October 2006. However, filtering for high confidence [Level 9] active fires, reduces this number to 6941 1kmx1km pixels. The respective measurements have 10%, median, and 90% values of FRP of [115,300,975] W/m^2 for all fires and [185,540,1495] W/m^2 for high confidence fires (**Table 3**). Overall, these values are much lower than FRP measured over other intensely burning regions [*Giglio et al.*, 2006]. However, the results are consistent with the fact that fires in the Maritime Continent occur under relatively wet surface conditions, due to high levels of mineral-soil moisture, extensive peat, and intermittent localized precipitation [*Couwenberg et al.*, 2010]. These results are based on more than 3000 daily MODIS fire hotspots and associated meteorological measurements.

There is only one day, October 2nd, with a statistically high FRP (daily mean more than monthly 90% value), for high confidence fires. Similarly, there are two days, October 28th and 30th, with an abnormally low FRP (daily mean less than monthly 15% value), for high confidence fires. None of these days have a statistically abnormal fire vertical height distribution. However, October 28th and 30th both show a sizable increase in AOD over the fire constrained region, with the AOD more than 2 standard deviations greater than the mean over the non fire constrained region, as compared to the period of time from the 25th through the 27th.One consistent rationale is that there was large-scale precipitation increasing aerosol removal and subsequently wetting the surface. This in turn led to lower temperature and FRP and

Deleted: significantly

Deleted:

Deleted: significant

Formatted: Font:

Deleted: significantly

Deleted: significantly

Deleted: significantly

Deleted: gnificant

correspondingly higher aerosol emissions factor on these days. Overall, there is no apparent impact of day-to-day variability of measured FRP driving observed variation in measured aerosol heights, and hence only high confidence fire data is subsequently used.

MERRA [Rienecker et al., 2011] reanalysis meteorology is used for the horizontal and vertical wind, and vertical temperature profile at each location where a fire is measured (**Table 3**). MERRA was chosen because it is based on NASA satellite measurements, and thus should be more consistent with the measurements used here. With the exceptions of October 5th and 20th, the horizontal wind is relatively calm 6.0 ± 1.3m/s. Also, throughout the entire month, the vertical temperature gradient is relatively stable -5.45 ± 0.16K/km, with only 7 individual fires occurring under unstable atmospheric conditions. Therefore, dynamical instability is not expected to contribute greatly to the vertical distribution [*Stone and Carlson*, 1979]. Also, the role played by the large-scale vertical wind is small 2.1 ± 1.6mm/s. Given the atmospheric stability and fire-controlled buoyancy conditions, the plume rise model approach should offer a reasonable approximation of the aerosol vertical distribution.

Deleted: significant

The approach used here relies upon the atmosphere being either stable or only minority non-stable. However, in general in this part of the world, there are two reasons that would contribute to most fires occurring under such conditions: firstly, that major instability would frequently lead to rain, fire suppression, and aerosol wash-out; and secondly that the induced surface cooling and atmospheric heating by the extensive aerosol layer itself would tend to increase the atmospheric stability. Such points are made clear in terms of the major unaccounted for processes in the MERRA data at this resolution, being: localized convection (due to the resolution), and the aerosol cooling and in-situ heating effects (not incorporated into MERRA's underlying model). In theory the direct and semi-direct effect may be able to be parameterized, but this would require a higher order model. Hence, since these conditions and effects are not considered by the plume rise model, they therefore cannot be explanations for discrepancies in the modeled vertical distribution.

3.3 Modeled Aerosol Vertical Distribution

Applying the plume rise model, the aggregated daily statistics of the vertical aerosol height at the bottom, lower-middle, median, upper-middle, and top are 0.60km, 1.14km, 1.85km, 2.87km, and 4.99km respectively (**Figure 4, Table 4**). The mean daily median, lower-middle, and bottom modeled heights are lower than the respective mean measured heights by 0.48km, 0.78km, and 1.07km respectively, with a wide underestimate day-to-day ranging from 1.91km to 1.11km. The upper-middle modeled height is about equal to measurements, with a mean difference of 0.03km, and wide day-to-day variations, from an overestimate of 1.97km to an underestimate of 1.36km. Finally, the top modeled heights are considerably higher than measurements, with an average overestimate of 1.02km, and a day-to-day range from an overestimate of 3.96km to an underestimate of 0.44km.

Deleted: significantly

The model underestimates the height of the median through bottom of the plume, while simultaneously overestimating the top. First, this means that the model is not accounting for enough energy to obtain the average rise of the plume. At the same time, the modeled vertical spread is too large, implying

other factors limit the height gain near the top of the plume while simultaneously enhance the height near the bottom. The results are consistent with one or both of the two hypothesized effects; first, that a low bias exists in the measured values of FRP [*Kahn et al.*, 2007; *Kahn et al.*, 2008], leading to insufficient buoyancy; and second, that in-situ stabilization occurs due to aerosol radiative cooling in the lower parts of the plume and aerosol radiative heating within the upper parts of the plume. This combination of factors is also consistent with the observed underestimate in measured FRP to match the median height, as well as the hypothesized complete non-detection of small fires [*Kaufman et al.*, 2003]. There are also uncertainties in the MERRA reanalysis products, but given the large sample size and the narrowness of the MERRA distribution, the impact of these uncertainties is considerably smaller than changes in the FRP on the order of 10%.

A sensitivity analysis is used to quantify the effects of a low bias in FRP, by applying a constant multiplicative factor to the measured FRP for each fire, from 1.0 to 2.0 in steps of 0.1 (although only the results in steps of 0.2 are given in **Table 4**). Although there are also uncertainties associated with measured vertical wind and temperature structure, this is not considered (**Table 3**), since there is no way to couple meteorological effects at sub-grid scale, or otherwise not included in the reanalysis meteorology. The results are obtained by minimizing the root-mean square (RMS) difference between the daily measured and modeled heights, for each FRP scaling factor, at each of the middle-upper, median, and middle-lower levels. The respective best-fit enhancement factors are **1.0** for middle-upper measurements (RMS=0.94km), **1.2** for median measurements (RMS=0.81km), and **2.0** for middle-lower measurements (RMS=0.74km) (**Table 4**). Although there is no single best-fit FRP scaling factor, the results produce a better fit to measured values from the middle-lower to the middle-upper than using the model without any FRP enhancement.

The results establish that current plume rise models can reproduce the median vertical plume height over Southeast Asia by increasing the FRP by 20%, a finding consistent with FRP generally underestimated over this region. By changing the FRP enhancement from 0% to 100%, the central height of the plume can be modeled, although the top and bottom heights of the plume cannot be reproduced. Additionally, the modeled plume is widely spread as compared to the narrowness of the measured plume. Unfortunately, rectifying these limitations will likely require the use of a more complex modeling approach and improvement of measured fire data.

There are additional errors associated with the non-complete complexity of the models employed. The models do not capture the contribution of atmospheric stabilization due to both the direct and semi-direct aerosol effects. Furthermore, these models do not take into account the impacts of localized convection. However, the majority of other works that employ regional and global models use this exact same methodology, and hence they also neglect these same small-scale phenomena in terms of communication between the chemistry, radiation, and the meteorology.

Formatted: Font:

4. Conclusions

This work comprehensively quantifies the significant present-day underestimation of the vertical distribution of aerosols over the Maritime Continent during an El-Nino influenced fire season, by introducing a new method to appropriately constrain the measurements over the geographical region of the aerosol plume. While this was a large-scale fire event, it was very special, because it occurred throughout the month of October, whereas typically the wet-season arrives sometime within the middle of the month. As such, the wetness of the soil and the large-scale meteorological flow, were both different this year from a more typical year. As a result, the measured heights over the constrained region are found to be higher than previously thought, with about 62% of aerosols found in the free troposphere, where they can be advected thousands of kilometers and have more impact on the atmospheric and climatic systems. Additionally, over the fire-constrained region, the vertical variability of the plume is found to be uniform throughout its height, implying that it is controlled mostly by local forcing, such as the buoyancy released by fires, localized convection, and aerosol/radiative feedbacks, such as the direct and semi-direct effects.

Application of a plume-rise model showed that there was an overall low bias against measured heights, which is consistent with the FRP being underestimated in this region of the world due to large-scale cloud cover. It was also determined that measured vertical heights are more narrowly confined than model simulations. Applying a robust sensitivity analysis found that the middle-lower through middle-upper extent of the plume can be reproduced if an appropriate (although changing) enhancement is applied to the FRP ranging from 1.0*FRP to 2.0*FRP (with 1.2*FRP the best fit-value). Hence, the variable FRP enhancement factor approach can allow for improved modeling of the height statistics for the middle-upper to middle-lower extent of the plume.

However, it is not possible to reproduce either the top or bottom of the measured heights, the knowledge of which is important to constrain the impacts of long-range transport and aerosol-climate interactions. Nor is it possible to reproduce the narrow spread of the measured heights. The results are consistent with the general understanding of current model shortcomings, which in addition to the underestimated FRP values, will also need to be addressed. Hence, the current community-wide dependence on FRP measurements for vertical aerosol modeling may lead to flaws in our being able to successfully model the distribution.

The results have been found to be robust over a region that behaves roughly uniformly over thousands of kilometers and includes regions both near and far from the source of the fires. Since there are only a few days that have relatively unique aerosol and meteorological properties over the period studied, the results support the most important aspect of improving the aerosol heights will be newer modelling approaches and improvements that will be able to resolve local-scale forcing, such as deep convection, aerosol/radiation interactions, and aerosol-cloud interactions. Secondly, the biased underestimation of FRP is also an important point to improve the aerosol height modeling, especially under conditions where cloudiness occurs or the measured AOD levels are very high. These errors are exacerbated over regions where large-scale precipitation is very low or where there is substantial aerosol/cloud intermixing. In all

Deleted: The

Deleted: significant

cases, until these model and measurement improvements are made, there is expected to be a significant underestimation of the aerosol loadings and radiative forcing distribution regionally, and to some extent globally. It is hoped that in the interim, the community will adapt a variable enhancement of FRP in tandem with measurement-constrained boundaries of smoke plumes, as a way to more precisely reproduce the statistics of the vertical aerosol distribution.

Acknowledgements:

We would like to acknowledge the PIs of the NASA MODIS, MISR, and CALIPSO projects for providing the data. The work was supported by the Chinese National Young Thousand Talents Program (Project 74110-52601113), and the Chinese Ministry of Science and Technology (Project 74110-41110002).

Deleted: financially

Deleted: of the Chinese National Government

Deleted: Project 74110-41110002 of

References:

Achtemeier, G., S. Goodrick, Y. Liu, F. Garcia-Menendez, Y. Hu, and M. Odman, (2011). Modeling smoke plume-rise and dispersion from Southern United States prescribed burns with daysmoke. Atmosphere, 2, 358-388.

Bjornsson, H. and Venegas, S, (1997). A Manual for EOF and SVD Analyses of Climate Data. Department of Atmospheric and Oceanic Sciences and Centre for Climate and Global Change Research, Tech. rep., McGill University, Technical Report, 1997.

Bond, T. C., D.G. Streets, K.F. Yarber, S.M. Nelson, J.H. Woo, and Z. Klimont. (2004). A technology-based global inventory of black and organic carbon emissions from combustion, J. Geophys. Res., 109, D14203, doi:10.1029/2003JD003697.

Briggs, G. A. (1965). A plume rise model compared with observations. *Journal of the Air Pollution Control Association*, vol. 15, no. 9, pp. 433–438.

Burnett, R., A. Pope, M. Ezzati, C. Olives, S. Lim, S. Mehta, H. Shin, G. Singh, B. Hubbell, M. Brauer, R. Anderson, K. Smith, J. Balmes, N. Bruce, H. Kan, F. Laden, A. Pruss-Ustun, M. Turner, S. Gapstur, R. Diver, and A. Cohen. (2014) An Integrated Risk Function for Estimating the Global Burden of Disease Attributable to Ambient Fine Particulate Matter Exposure, Environ Health Perspect; doi:10.1289/ehp.1307049.

Campbell, J.R., Reid, J.S., Westphal, D.L., Zhang, J.L., Tackett, J.L., Chew, B.N., Welton, E.J., Shimizu, A., Sugimoto, N., Aoki, K., Winker, D.M. (2013) Characterizing the vertical profile of aerosol particle extinction and linear depolarization over Southeast Asia and the Maritime Continent: The 2007–2009 view from CALIOP, Atmospheric Research, 122, March 2013, 520–543, http://dx.doi.org/10.1016/j.atmosres.2012.05.007.

Chew, B. N., J.R. Campbell, S.V. Salinas, C.W. Chang, J.S. Reid, E.J. Welton, and S.C. Liew. (2013). Aerosol particle vertical distributions and optical properties over Singapore. *Atmospheric Environment*, *79*, 599-613.

Chung, C. E., V. Ramanathan and D. Decremer. (2012) Observationally constrained estimates of carbonaceous aerosol radiative forcing, *Proc. Natl. Acad. Sci. U.S.A.*, doi:10.1073/pnas.1203707109.

Cohen, J. B. and Prinn, R. G. (2011). Development of a fast, urban chemistry metamodel for inclusion in global models, Atmos. Chem. Phys., 11, 7629–7656, doi:10.5194/acp-11-7629-2011.

Cohen, J. B. (2014) Quantifying the occurrence and magnitude of the Southeast Asian fire climatology. *Environmental Research Letters*, *9*(11), 114018.

Cohen, J. B., Lecoeur, E., and Hui Loong Ng, D. (2017) Decadal-scale relationship between measurements of aerosols, land-use change, and fire over Southeast Asia, Atmos. Chem. Phys., 17, 721-743, doi:10.5194/acp-17-721-2017.

Cohen, J. B. and Wang C (2014) Estimating Global Black Carbon Emissions Using a Top-Down Kalman Filter Approach. *J. Geophys. Res.*, doi:10.1002/2013JD019912.

Deleted:

Formatted: Not Highlight

Deleted:

Deleted: :

Deleted: , 2017

Colarco, P., M. Schoeberl, B. Doddridge, L. Marufu, O. Torres, and E. Welton. (2004) Transport of smoke from Canadian forest fires to the surface near Washington, D.C.: Injection height, entrainment, and optical properties, *J. Geophys. Res.*, 109, D06203, doi:10.1029/2003jd00424.

Couwenberg, J., R. Dommain, and H. Joosten, H. (2010). Greenhouse gas fluxes from tropical peatlands in south-east Asia. Global Change Biology, 16: 1715–1732. doi:10.1111/j.1365-2486.2009.02016.

Delene, D. J. and J.A. Ogren (2002) Variability of aerosol optical properties at four North American surface monitoring sites, J. Atmos. Sci., 59(6), 1135–1150.

Dennis, R. A., J. Mayer, G. Applegate, U. Chokkalingam, C.J.P. Colfer, I. Kurniawan, and T.P. Tomich. (2005). Fire, people and pixels: linking social science and remote sensing to understand underlying causes and impacts of fires in Indonesia. *Human Ecology*, *33*(4), 465-504.

Dubovik, O., A. Smirnov, B.N. Holben, M.D. King, Y.J. Kaufman, T.F. Eck and I Slutsker. (2000) Accuracy assessments of aerosol optical properties retrieved from Aerosol Robotic Network (AERONET) Sun and sky radiance measurements. J. Geophys. Res., 105(D8), 9791-9806.

Ekman, A., A. Engstrom and C. Wang. (2007). The effect of aerosol composition and concentration on the development and anvil properties of a continental deep convective cloud, Q. J. Roy. Meteor. Soc., 133B(627), 1439-1452.

Ekman, A. M. L., M. Hermann, P. Gross, J. Heintzenberg, D. Kim, and C. Wang. (2012). Sub-micrometer aerosol particles in the upper troposphere/lowermost stratosphere as measured by CARIBIC and modeled using the MIT-CAM3 global climate model, *J. Geophys. Res*., 117, D11202, doi:10.1029/2011JD016777.

Field, R. D., G.R. van der Werf, S.P.P. Shen. (2009) Human amplification of drought-induced biomass burning in Indonesia since 1960. *Nature Geosci.*, 10.1038/ngeo443.

Freeborn, P. H., M.J. Wooster, D.P. Roy and M.A. Cochrane. (2014). Quantification of MODIS fire radiative power (FRP) measurement uncertainty for use in satellite-based active fire characterization and biomass burning estimation, *Geophys. Res. Lett.*, 41, 1988–1994, doi:10.1002/2013GL59086.

Giglio, L., I. Csiszar and C.O. Justice. (2006) Global distribution and seasonality of active fires as observed with the Terra and Aqua MODIS sensors. *J. Geophys. Res.*, doi:10.1029/2005JG000142.

Hansen, M. C. (2008). Humid tropical forest clearing from 2000 to 2005 quantified by using multitemporal and multiresolution remotely sensed data. Proc. Natl. Acad. Sci. USA, 105, 9439–9444.

Hostetler, C., Hair, J., Liu, Z.Y., Ferrare, R., Harper, D., Cook, A., Vaughan, M., Trepte, C., Winker. D. (2008) Validation of CALIPSO Lidar Observations Using Data From the NASA Langley Airborne High Spectral Resolution Lidar (Retrieved from: https://ntrs.nasa.gov/archive/nasa/casi.ntrs.nasa.gov/20080014234.pdf)

Hostetler, C, Z. Liu, J. Reagan, M. Vaughan, D. Winker, M. Osborn, W. Hunt, K. Powell, and C. Trepte. (2006). CALIOP Algorithm Theoretical Basis Document–Part 1: Calibration and Level 1 Data Products. *Doc. PC-SCI* 201.

Jchoku, C., L. Giglio, M. Wooster and L. Remer. (2008). Global characterization of biomass-burning

Deleted:

patterns using satellite measurements of fire radiative energy. *Remote Sensing of Environment* 112.6, 2950-2962.

Kahn, R.A., Chen, Y., Nelson, D.L., Leung, F.Y., Li, Q.B., Diner, D.J., and Logan, J.A. (2008). Wildfire smoke injection heights: Two perspectives from space. *Geophys. Res. Lett.*, 35, L04809, doi:10.1029/2007GL032165.

Kahn, R.A., Li, W.H., Moroney, C., Diner, D.J., Martonchik, J.V., and Fishbein, E. (2007). Aerosol source plume physical characteristics from space-based multiangle imaging. *J. Geophys. Res.*, 112, D11205, doi:10.1029/2006JD007647, 2007

Kalnay et al. (1996). The NCEP/NCAR 40-year reanalysis project, Bull. Amer. Meteor. Soc., 77, 437-470.

Kaufman, Y. J., C. Ichoku, L. Giglio, S. Korontzi, D.A. Chu, W.M. Hao, and C.O. Justice. (2003). Fire and smoke observed from the Earth Observing System MODIS instrument--products, validation, and operational use. *International Journal of Remote Sensing*, *24*(8), 1765-1781.

Kim, D., C. Wang, A.M.L. Ekman, M. C. Barth, and P. Rasch. (2008) Distribution and direct radiative forcing of carbonaceous and sulfate aerosols in an interactive size-resolving aerosol-climate model, *J. Geophys. Res*., 113, D16309, doi:10.1029/2007JD009756.

Lamarque, J. F. (2010). Historical (1850–2000) gridded anthropogenic and biomass burning emissions of reactive gases and aerosols: methodology and application. *Atmos. Chem. Phys.*, doi:10.5194/acp-10-7017-2010.

Langmann, B., B. Duncan, C. Textor, J. Trentmann, and G.R. van der Werf. (2009). Vegetation fire emissions and their impact on air pollution and climate. *Atmospheric Environment*, *43*(1), 107-116.

Lee, J., Hsu, N.C., Bettenhausen, C., Sayer, A.M., Seftor, C.J., Jeong, M.J., Tsay, S.C., Welton, E.J., Wang, S.H., Chen, W.N. (2016) Evaluating the Height of Biomass Burning Smoke Aerosols Retrieved from Synergistic Use of Multiple Satellite Sensors over Southeast Asia, Aerosol and Air Quality Research, 16: 2831–2842 doi:10.4209/aaqr.2015.08.0506

Leung, F.Y.T., J.A. Logan, R. Park, E. Hyer, E. Kasischke, D. Streets, and L. Yurganov. (2007) Impacts of enhanced biomass burning in the boreal forests in 1998 on tropospheric chemistry and the sensitivity of model results to the injection height to emissions. *J. Geophys. Res.*, 112, D10313, doi:10.1029/2006JD008132.

Lin, N. H., A.M. Sayer, S.H. Wang, A.M. Loftus, T.C. Hsiao, G.R. Sheu, and S. Chantara. (2014). Interactions between biomass-burning aerosols and clouds over Southeast Asia: Current status, challenges, and perspectives. *Environmental Pollution*, *195*, 292-307.

Martin, V.M., R.A. Kahn, J.A. Logan, R. Paugam, M. Wooster, and C. Ichoku. (2012). Space-based observational constraints for 1-D fire smoke plume-rise models. *Journal of Geophysical Research: Atmospheres (1984–2012)*, *117*(D22).

Miettinen, J., E. Hyer, A.S. Chia, L.K. Kwoh, and S.C. Liew, S. C. (2013). Detection of vegetation fires and burnt areas by remote sensing in insular Southeast Asian conditions: current status of knowledge and future challenges. *International journal of remote sensing*, *34*(12), 4344-4366.

Ming, Y., V. Ramaswamy and G. Persad. (2010) Two opposing effects of absorbing aerosols on global-mean precipitation. *Geophysical Research Letters* 37.13.

Nakajima, T., A. Higurashi, N. Takeuchi and J.R. Herman (1999). Satellite and ground-based study of optical properties of 1997 Indonesian Forest Fire aerosols. Geophys. Res. Lett., 10.1029/1999GL900208.

Petersen, W. and S. Rutledge. (2001). Regional Variability in Tropical Convection: Observations from TRMM. J. Climate, 14, 3566–3586.

Petrenko, M., R.A. Kahn, M. Chin, A.J. Soja, T. Kucsera, and Harshvardhan. (2012) The use of satellite-measured aerosol optical depth to constrain biomass burning emissions source strength in the global model GOCART, *J. Geophys. Res.*, doi:10.1029/2012JD01787.

Rienecker, M.M., M.J. Suarez, R. Gelaro, R. Todling, J. Bacmeister, E. Liu, M.G. Bosilovich, S.D. Schubert, L. Takacs, G.-K. Kim, S. Bloom, J. Chen, D. Collins, A. Conaty, and A. da Silva (2011). MERRA: NASA's Modern-Era Retrospective Analysis for Research and Applications. J. Climate, 24, 3624-3648, doi:10.1175/JCLI-D-11-00015.1

Rogers, R.R., Hostetler, C.A., Ferrare, R.A., Hair, J.W., Obland, M.D., Cook, A.L., Harper, D.B., Swanson, A.J. (2009) Validation of CALIOP Aerosol Backscatter and Extinction Profile Products Using Airborne High Spectral Resolution Lidar Data (Retrieved from: http://cimss.ssec.wisc.edu/calipso/meetings/cloudsat_calipso_2009/Posters/Rogers.pdf)

Schuster, G. L., O. Dubovik, B. Holben and E. Clothiaux. (2005) Inferring black carbon content and specific absorption from Aerosol Robotic Network (AERONET) aerosol retrievals, *J. Geophys. Res.*, 110, D10S17, doi:10.1029/2004JD004548.

Sessions, W. R., H.E. Fuelberg, R.A. Kahn, and D.M. Winker. (2011). An investigation of methods for injecting emissions from boreal wildfires using WRF-Chem during ARCTAS. *Atmospheric Chemistry and Physics*, *11*(12), 5719-5744.

Sofiev, M., T. Ermakova, and R. Vankevich. (2012). Evaluation of the smoke-injection height from wildland fires using remote-sensing data. *Atmos. Chem. Phys*, vol. 12, no. 4, pp. 1995–2006.

Stone, P. and J. Carlson. (1979). Atmospheric Lapse Rate Regimes and Their Parameterization. J. Atmos. Sci., 36, 415–423.

Sugimoto, N., Nishizawa T., Shimizu A., Matsui I., Jin Y. (2014) Characterization of aerosols in East Asia with the Asian dust and aerosol lidar observation network (AD-Net) Proc. SPIE 9262 92620K

Sugimoto, N., Shimizu, A., Nishizawa, T., Matsui, I., Jin, Y., Khatri, P., Irie, H., Takamura, T., Aoki, K., Thana, B. (2014) Aerosol characteristics in Phimai, Thailand determined by continuous observation with a polarization sensitive Mie–Raman lidar and a sky radiometer, Environmental Research Letters, 10, 6.

Tao, W.K., J.P. Chen, Z.Q. Li, C. Wang, and C.D. Zhang. (2012) The Impact of Aerosol on convective cloud and precipitation. *Rev. Geophys*., 50, RG2001, doi:10.1029/2011RG000369.

Taylor, D. (2010). Biomass burning, humans and climate change in Southeast Asia. *Biodiversity and*

Deleted:

Formatted: No widow/orphan control

conservation, *19*(4), 1025-1042.

Tosca, M. G., J.T. Randerson, C.S. Zender, D.L. Nelson, D.J. Diner, and J.A. Logan (2011), Dynamics of fire plumes and smoke clouds associated with peat and deforestation fires in Indonesia, *J. Geophys. Res*., 116, D08207, doi:10.1029/2010JD015148.

Tsigaridis, K., N. Daskalakis, M. Kanakidou, P.J. Adams, P. Artaxo, R. Bahadur, Y. Balkanski, S.E. Bauer, N. Bellouin, A. Benedetti, T. Bergman, T.K. Berntsen, J.P. Beukes, H. Bian, K.S. Carslaw, K. S., M. Chin, G. Curci, T. Diehl, R.C. Easter, S.J. Ghan, S.L., Gong, A. Hodzic, C.R. Hoyle, T. Iversen, S. Jathar, J.L. Jimenez, J.W. Kaiser, A. Kirkevag, D. Koch, H. Kokkola, Y.H. Lee, G. Lin, X. Liu, C. Luo, X. Ma, G.W. Mann, N. Mihalopoulos, J.J. Morcrette, J.F. Müller, G. Myhre, S. Myriokefalitakis, N.L. Ng, D. O'Donnell, J.E. Penner, L. Pozzoli, K.J. Pringle, L.M. Russell, M. Schulz, J. Sciare, O. Seland, D.T. Shindell, S. Sillman, R.B. Skeie, D. Spracklen, T. Stavrakou, S.D. Steenrod, T. Takemura, P. Tiitta, S. Tilmes, H. Tost, T. van Noije, P.G. van Zyl, K. von Salzen, F. Yu, Z. Wang, Z. Wang, R.A. Zaveri, H. Zhang, K. Zhang, Q. Zhang, and X. Zhang, X. (2014) The AeroCom evaluation and intercomparison of organic aerosol in global models, Atmos. Chem. Phys., 14, 10845-10895, doi:10.5194/acp-14-10845-2014.

van der Werf, G. R. (2010). Global fire emissions and the contribution of deforestation, savanna, forest, agricultural, and peat fires (1997–2009). *Atmos. Chem. Phys.*, 10.5194/acp-10-11707-2010.

van der Werf, G. R., J. Dempewolf, S.N. Trigg, J.T. Randerson, P.S. Kasibhatla, L. Giglio, and R.S DeFries. (2008). Climate regulation of fire emissions and deforestation in equatorial Asia. *Proceedings of the National Academy of Sciences*, *105*(51), 20350-20355.

Wang, C. (2013) Impact of anthropogenic absorbing aerosols on clouds and precipitation: A review of recent progresses, *Atmos. Res*., 122, 237-249.

Wang, C. (2007). Impact of direct radiative forcing of black carbon aerosols on tropical convective precipitation, Geophys. Res. Lett., 34, L05709, doi:10.1029/2006GL028416.

Winker, D. M., J. Pelon, and M.P. McCormick (2003), The CALIPSO mission: Spaceborne lidar for observation of aerosols and clouds, *Proc. SPIE*, **4893**, 1–11.

Woodward J. L. (2010). *Estimating the Flammable Mass of a Vapour Cloud: A CCPS Concept Book*, John Wiley & Sons, ISBN 0470935359, 9780470935354.

Wooster, M. J., G.L.W. Perry and A. Zoumas. (2012) Fire, drought and El Niño relationships on Borneo (Southeast Asia) in the pre-MODIS era (1980–2000), Biogeosciences, 9, 317-340, doi:10.5194/bg-9-317-2012.

635 **Table 1**: Statistical summary of measured (CALIPSO) smoke plume heights in October 2006, at different
636 percentiles of extinction height (top/Z=10%, middle-upper/ Z=30%, median/Z=50%, middle-lower/Z=70%,
637 and bottom/Z=90%), over the subset of the Maritime Continent **impacted by smoke** (**FIRE**), and **not**
638 **impacted by smoke** (**NO-FIRE**), based on MISR observations (**Figure 1).** "MEAN" is average, "STD" is
639 standard deviation, and percentages XX% are the corresponding distribution's percentiles. Days which are
640 statistical outliers (mean >**85%** or <**15%** of at least one variable) are listed as **1st**, **3rd**, etc.

	bottom [km]	middle-lower [km]	median [km]	middle-upper [km]	top [km]
FIRE 5%	0.18	0.36	0.56	0.89	1.31
FIRE 10%	0.25	0.49	0.76	1.09	1.53
FIRE 15%	0.31	0.59	0.92	1.29	1.67
FIRE 50%	1.38	1.59	1.83	2.22	2.82
FIRE 85%	2.75	2.92	3.13	3.37	3.70
FIRE 90%	3.14	3.30	3.45	3.72	4.07
FIRE 95%	4.18	4.38	4.70	5.56	5.65
FIRE MEAN	1.68	1.92	2.17	2.50	2.98
FIRE STD	1.59	1.55	1.53	1.54	1.55
NO-FIRE 5%	0.16	0.33	0.48	0.60	0.70
NO-FIRE 10%	0.19	0.38	0.55	0.68	0.87
NO-FIRE 15%	0.21	0.42	0.59	0.77	1.12
NO-FIRE 50%	0.31	0.57	0.83	1.25	1.76
NO-FIRE 85%	1.16	1.64	2.01	2.36	2.85
NO-FIRE 90%	1.65	1.98	2.27	2.60	3.05
NO-FIRE 95%	2.22	2.45	2.73	2.99	3.41
NO-FIRE MEAN	0.97	0.98	1.00	1.02	1.08
NO-FIRE STD	0.65	0.93	1.21	1.53	1.98

641

642 **Table 2**: Summary of measured (CALIPSO) smoke plume heights in October 2006, for days that are
643 statistical outliers **mean (>85% or <15%) of all data in bold**, mean (>80% or <20%) of all data in regular
644 text. The levels are given as a percentile of extinction height over the subset of the Maritime Continent
645 **impacted by smoke** (fire-constrained), based on MISR observations (**Figure 1).**

	bottom (90% Extinction) [km]	middle-lower (70% Extinction) [km]	median (50% Extinction) [km]	middle-upper (30% Extinction) [km]	top (10% Extinction) [km]
FIRE 11th	2.29	2.54	**3.26**	**4.11**	**4.93**
FIRE 15th	1.85	2.20			
FIRE 22nd	**2.55**	**2.85**	2.95		

646

Table 3: Monthly statistics of measured fire properties (FRP and T_F), for all measured fires (**ALL**) and level 9 confidence fires (**L9**) and MERRA meteorological properties (T_A, v, U, dT/dz) corresponding to the geographic locations of **L9**. All data is constrained by the boundaries of the fire extent in October 2006 (**Figure 1**). The distribution's percentile is given as "**XX%**", the mean and standard deviation are given as "**MEAN**" and "**STD**". Note that there were no observed fires of L9 on the following dates: 17th, 22nd, 23rd, 24th, 25th, 26th, 27th, 29th, 31st.

	FRP **ALL** [W/m^2]	FRP **L9** [W/m^2]	T_F **ALL** [K]	T_F **L9** [K]	T_A **L9** [K]	V **L9** [mm/s]	U **L9** [m/s]	dT/dz **L9** [K/km]
5%	95.	140.	370.	410.	296.0	0.2	4.1	-5.25
10%	115.	185.	390.	445.	296.4	0.4	4.4	-5.27
15%	130.	230.	400.	480.	296.6	0.6	4.5	-5.28
50%	300.	540.	535.	725.	298.4	1.5	6.0	-5.43
85%	775.	1240.	910.	1275.	301.1	4.1	7.4	-5.65
90%	975.	1495.	1070.	1525.	301.5	4.6	7.7	-5.69
95%	1290.	1855.	1335.	1850.	302.1	5.6	8.1	-5.75
Mean	510.	920.	702.	1029.	298.7	2.1	6.0	-5.44
StD	720.	1340.	573.	1057.	2.0	1.6	1.3	0.16

Table 4: Monthly statistics of modeled aerosol heights, based upon level 9 confidence fires (**L9**) and MERRA meteorological properties (T_A, v, U, dT/dz) at the corresponding geographic locations. Sensitivity tests are shown with their respective weighting factor (**1.2, 1.4, 1.6, 1.8, or 2.0**) applied to the measured FRP. The modeled heights are given by percentile from the bottom (5%) to the top (95%), while the mean and standard deviation are given as "**MEAN**" and "**STD**". Note that the model was not run on the following days, during which there were no observed **L9** fires: 17th, 22nd, 23rd, 24th, 25th, 26th, 27th, 29th, and 31st.

	FRP(x1.0) [km]	**FRP(x1.2) [km]**	**FRP(x1.4) [km]**	**FRP(x1.6) [km]**	**FRP(x1.8) [km]**	**FRP(x2)[km]**
5%	**0.41**	0.44	0.48	0.53	0.56	0.60
10%	**0.60**	0.67	0.73	0.80	0.85	0.91
15%	**0.75**	0.83	0.91	0.98	1.05	1.12
30%	**1.14**	1.28	1.40	1.52	1.63	1.74
50%	**1.85**	2.07	2.27	2.47	2.65	2.82
70%	**2.87**	3.23	3.54	3.84	4.12	4.38
85%	**4.21**	4.66	5.11	5.53	5.87	6.22
90%	**4.99**	5.54	6.08	6.58	6.97	7.41
95%	**6.10**	6.79	7.43	7.76	8.16	8.61
Mean	**2.41**	2.69	2.96	3.21	3.44	3.67
StD	**1.98**	2.21	2.42	2.62	2.81	2.99

Figure 1: Map of Maritime Continent. The smoke plume impacts the sub-region contained within the dashed lines, or the so-called **fire-constrained** region. On the other hand, the region outside of the dashed lines is the so-called **non fire-constrained** region. The plot is based on a variance maximization technique applied to the measurements from all MISR overpasses from 2000 through 2014 (*Cohen*, 2014). Note that in this part of the world 1 degree of latitude or longitude is approximately 100km, leading to a fire-impacted region over 2500km across.

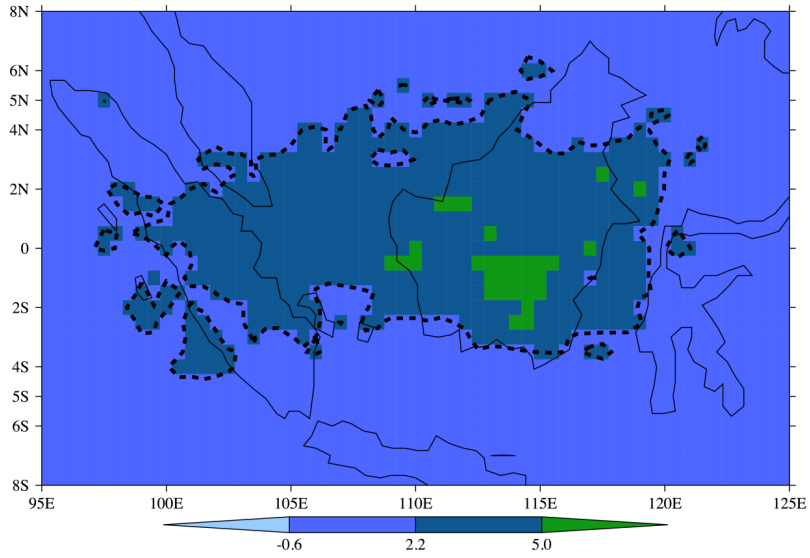

Figure 2a,2b: Time series of measured CALIPSO extinction heights over the fire constrained (A) and non fire-constrained (B) regions as given **Figure 1**. For both plots, the dots correspond to the height of the column integrated backscatter at: 10% [red] (top), 30% [dark blue], 50% [yellow], 70% [black], and 90% [light blue] (bottom). The circles are computed daily means, while dots are the computed daily standard deviation bands. There was no measurement over the region on the 10th, 16th, and 20th.

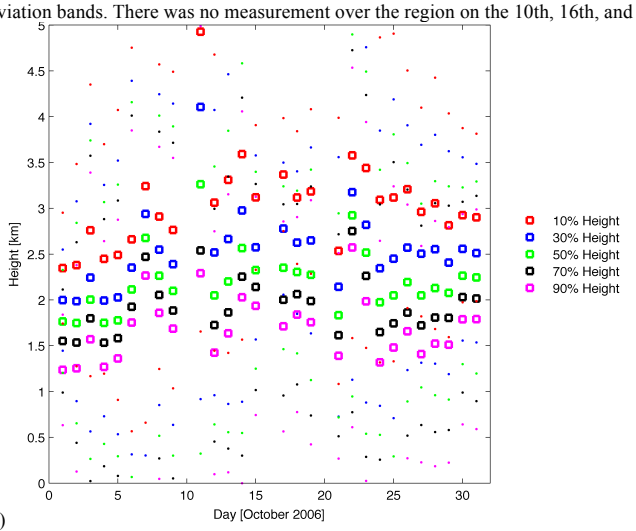

(A)

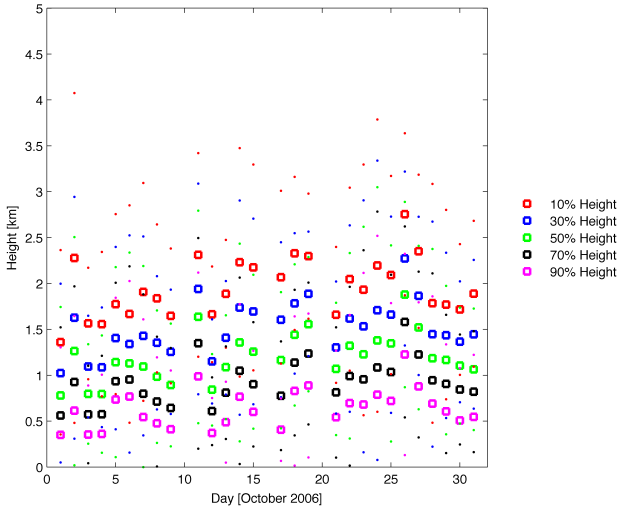

(B)

Figure 3: Time series of daily averaged measured AOD over the fire-constrained regions of the Maritime Continent [blue], and the non fire-constrained regions of the Maritime Continent [red], as given in **Figure 1**. Circles are computed daily mean values, while dots are computed daily standard deviation bands.

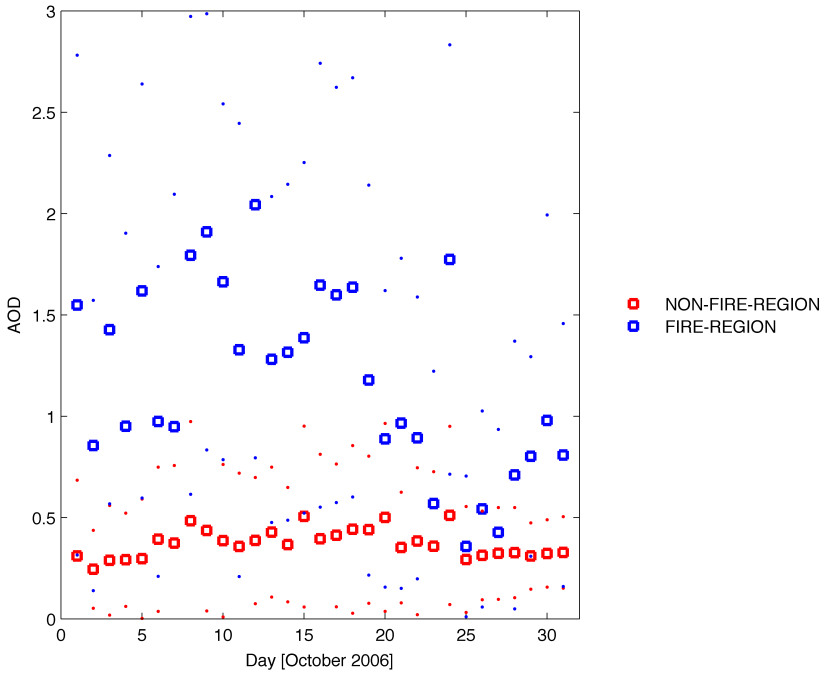

Figure 4: Time series of PDFs (20% and 80% values are stars and mean values are given by lines) of the measured extinction heights for middle-upper (blue), median (red), and middle-lower (green) levels. The best fitting modeled heights are given as 0% FRP enhancement (solid black line) (best fit for middle-upper measurements), 20% FRP enhancement (dashed black line) (best fit for median measurements), and 100% FRP enhancement (dotted black line) (best fit for the middle-lower measurements).

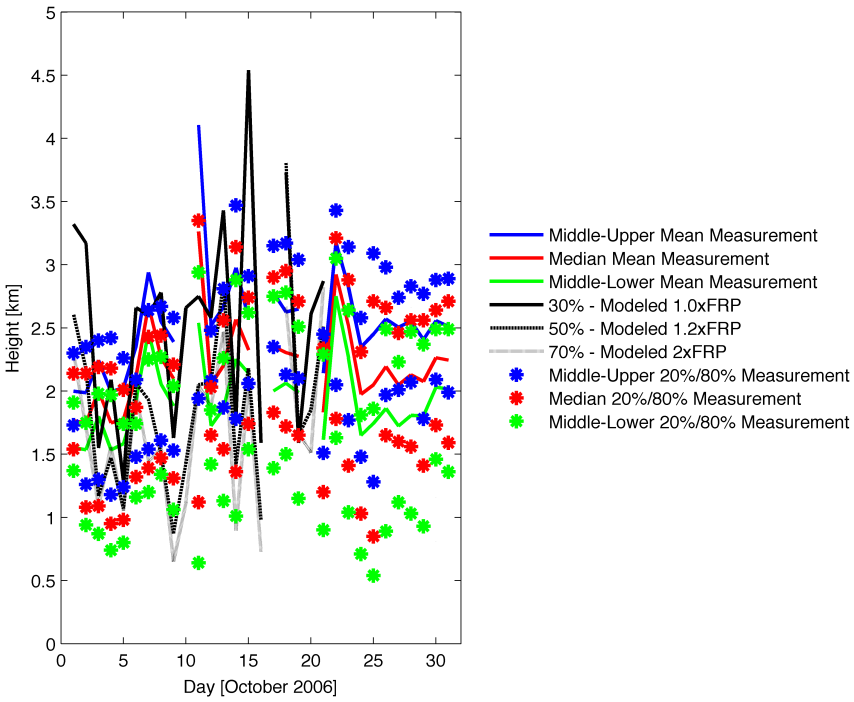

Response to Reviewer Number 1:

We thank reviewer number 1 for his/her comments. There are some constructive comments. Especially in terms of the uncertainties in the boundary layer heights being made more prominent and in terms of uncertainties in the lidar measurements being more carefully examined. Furthermore, there are multiple suggestions for improving wording, and for making clear when statistical significance is used, as compared to other comparisons. We appreciate these suggestions.

However, we want to emphasize that in fact, this work is a significant advance compared to other works in the literature. We hope to demonstrate that this work is up to date in terms of calibration, new in scope, and provides some major advances of interest to the larger community:

One of the most comprehensive papers with respect to CALIOP over Southeast Asia, is given by Lee et al. [2016] (plus an entire team associated with NASA). They published a paper using CALIOP data over Southeast Asia, using slightly less error quantification for high ice clouds found in the tropics [although they may have done this from the way they configure figure 3, but it is not explicitly mentioned], which we have employed. Additionally, they used products that we knew are less reliable, such as SSA, and assumed that they were extendable functionally as the backscatter ratio goes (which is not necessarily a good assumption, but is certainly a much weaker assumption than we use in equating heights to backscatter). We made sure to stick to only the most reliable product, backscatter, as is also demonstrated in more depth by Rogers et al. [2009] and Hostetler [2008]. Furthermore, we performed the exact thing that these papers identified as the major weakness of CALIOP data, a methodology of how to combine the spatially-disparate paths, into a useful contiguous product.

As can be seen in the literature, many other papers use CALIOP without any validation at all [Sugimoto et al., 2015], or actually use it to validate models, which are known to themselves be highly inaccurate. This can be seen by the many papers put put by Jeff Reid and his team, whereby NAAPS (A modeling system) is used to validate CALIOP [Campbell et al., 2013]. A quick look at their most important validation for the NAAPS model (supplemental figure 6) shows that it performs less well than the modeling system (Cohen, 2014; Cohen and Wang, 2014; Cohen et al., 2017) over this region during the biomass burning season, since the annual average values still perform only as well, and due to the biases included within. Furthermore, as already demonstrated in the paper's references, the results are very comparable with findings from Lin Neng-Hui's group in Taiwan [Lin et al, 2014, 2013, etc.], and the AD-Net [Sugimoto et al, 2014] who are making observations with on-the-ground lidar at multiple places within the Northern portion of Southeast Asia and Greater East Asia. Hence, it should be completely reasonable to assume that the validation against the results and findings from the underlying measurements, upon which those results are based, should be sufficient validation.

In an ideal world, there would be more validation on the ground in this region. However, this team, and many others are work to continue to improve this situation as best as possible. If there are any specific comparisons that you could recommend to

continue to demonstrate the uniqueness of this result and its strength, compared to the other papers currently available, please let us know. From what we can see, this is the only paper that is comprehensive in its analysis on a day-by-day basis over a long-term such fire event, looking carefully over its total spatial extent over this region, not merely hunting for or tracing a few daily events, or randomly sampling over a very long spatial/temporal extent which is mixing both fire and non-fire type of atmospheric conditions.

Many of the other comments in terms of validating the errors of the models and measurements are mentioned in the other response and will not be repeated here. However, we take these suggestions very seriously and look forward to work with the reviewer to address their concern of the newness and significance of the results.

Finally, we agree that more information can be provided, and hope to do this by producing a probability distribution function of the results, on a day-by-day basis as well as over the entire month, for both the measurements and the models, and will include a summary as a new figure, with the remainder placed in appendices. We hope that this can address and demonstrate the significant importance, especially given the fact that the actual, stabilized boundary layer, may be lower than the 1000m as measured over Singapore.

References:

Campbell, J.R., Reid, J.S., Westphal, D.L., Zhang, J.L., Tackett, J.L., Chew, B.N., Welton, E.J., Shimizu, A., Sugimoto, N., Aoki, K., Winker, D.M. (2013) Characterizing the vertical profile of aerosol particle extinction and linear depolarization over Southeast Asia and the Maritime Continent: The 2007–2009 view from CALIOP, Atmospheric Research, 122, March 2013, 520–543, http://dx.doi.org/10.1016/j.atmosres.2012.05.007.

Hostetler, C., Hair, J., Liu, Z.Y., Ferrare, R., Harper, D., Cook, A., Vaughan, M., Trepte, C., Winker. D. (2008) Validation of CALIPSO Lidar Observations Using Data From the NASA Langley Airborne High Spectral Resolution Lidar (Retrieved from: https://ntrs.nasa.gov/archive/nasa/casi.ntrs.nasa.gov/20080014234.pdf)

Lee, J., Hsu, N.C., Bettenhausen, C., Sayer, A.M., Seftor, C.J., Jeong, M.J., Tsay, S.C., Welton, E.J., Wang, S.H., Chen, W.N. (2016) Evaluating the Height of Biomass Burning Smoke Aerosols Retrieved from Synergistic Use of Multiple Satellite Sensors over Southeast Asia, Aerosol and Air Quality Research, 16: 2831–2842 doi:10.4209/aaqr.2015.08.0506

Rogers, R.R., Hostetler, C.A., Ferrare, R.A., Hair, J.W., Obland, M.D., Cook, A.L., Harper, D.B., Swanson, A.J. (2009) Validation of CALIOP Aerosol Backscatter and Extinction Profile Products Using Airborne High Spectral Resolution Lidar Data (Retrieved from: http://cimss.ssec.wisc.edu/calipso/meetings/cloudsat_calipso_2009/Posters/Rogers.pdf)

Sugimoto, N., Nishizawa T., Shimizu A., Matsui I., Jin Y. (2014) Characterization of aerosols in East Asia with the Asian dust and aerosol lidar observation network (AD-Net) Proc. SPIE 9262 92620K

Sugimoto, N., Shimizu, A., Nishizawa, T., Matsui, I., Jin, Y., Khatri, P., Irie, H., Takamura, T., Aoki, K., Thana, B. (2014) Aerosol characteristics in Phimai, Thailand determined by continuous observation with a polarization sensitive Mie–Raman lidar and a sky radiometer, Environmental Research Letters, 10, 6.

Response to Reviewer Number 2:

We thank reviewer number 2 for his/her comments. There are some constructive comments. Additionally, some of the comments show indirectly that the wording should be improved for clarity, as part of the structure of the way the research was organized was possibly misunderstood.

However, we strongly urge the reviewer to be more careful, and to actually read the paper to the end. The reason being that a few of the points made, including stating that the data was "inadequate" to "support the scientific conclusions", were actually already addressed in the paper, through figures and tables.

These details will be given below in the point-by-point response. Reviewer comments are preceded by RC: and are *italicized*, while the author responses are preceded by AC:

RC: "Authors didn't mention about the aerosol-retrieval uncertainties over the land, especially during large-scale fire events"
AC: This has been mentioned in other papers we have cited and already performed over this region (Cohen, 2014; Cohen et al., 2017). However, for clarity the values will be added into this paper. There are two issues, the first with cloud cover, in which a bias may exist because extremely high AOD conditions (AOD>2) are frequently flagged as clouds. The second is the error itself over land, which can go as high as 15%. However, as you can see from the figures and the tables, the difference between the "fire region" and the "non-fire region" is significant at values where the errors are much larger than 15%. This has already been factored in, but will be made clear. The terms of the issues of the bias by cloud screening reducing the measured AOD is if anything a stronger supporting issue for the results given here, since it would make the difference between the "fire region" and the "non-fire region" even larger. It is also the reason why MISR was used for the initial definition of the two regions, since its ability to cloud clear is better than MODIS over this region. It is furthermore a point of interest when analyzing the CALIOP data, which has some ability to distinguish between aerosol and cloud. There is discussion of this in Section 2.2 and it can be expanded.

RC: "How good are MODIS and MISR retrievals over Southeast Asia?"
AC: This has been mentioned in other papers we have cited and already preformed over this region (Cohen, 2014; Cohen et al., 2017). In general, these products need to be used carefully, but the relationships found, when applying the techniques outlined here and in previous work, match extremely well with ground measurements from AERONET, within the errors of the 15% stated above. Additionally, model results forced with these measurements, have been shown to match very well with NOAA, Chinese, and other networks downwind throughout Southeast and East Asia. Additional comparisons about this can be included. And these matches have been demonstrated over not only the time period of this paper, but for the past decade. There are many errors using the satellite data, but the errors are sufficiently small as to not impact the analysis when looking at the events outlined here, due to their intense magnitude and spatial extent. There is discussion of this in Section 2.2 and it can be expanded.

RC: "What is the mean AOD observed during the fire events?"

AC: This was clearly something that the reviewer missed. I urge the reviewer to carefully look at **Figure 3** and the text on lines 132-138. I am attaching them for reference:

Figure 3: Time series of daily averaged measured AOD over the fire-constrained regions of the Maritin Continent [blue], and the non fire-constrained regions of the Maritime Continent [red], as given in **Figu 1**. Circles are computed daily mean values, while dots are computed daily standard deviation bands.

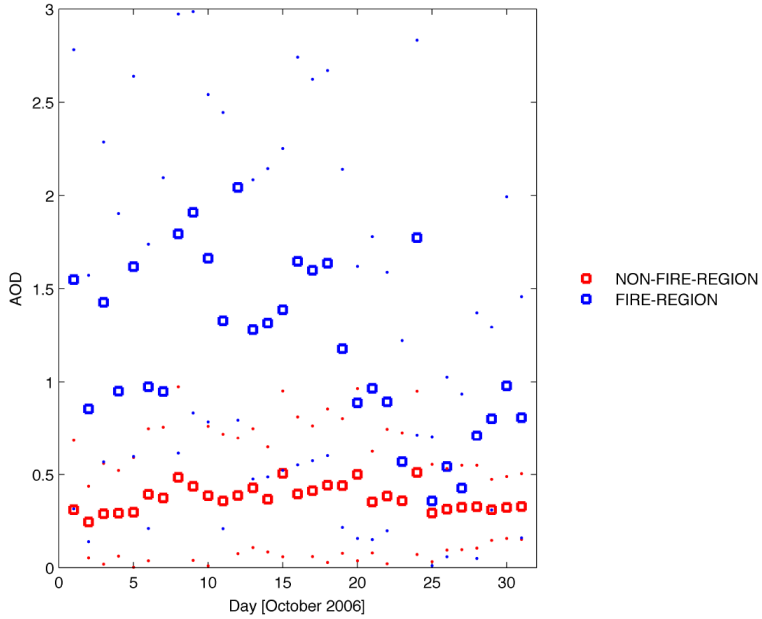

---

et al., 2007]. On the other hand, while some grids are contaminated, the sheer spatial distance of the plume and the fact that the overwhelming majority of atmospheric aerosols during this time of the year are due to fires, means that there is no significant bias in the overall statistics of the measured AOD [*Cohen*, 2014], as observed by looking at the spatially averaged MODIS AOD and statistics over the fire-constrained and non fire-constrained regions (**Figure 3**). The AOD is significantly higher ($p<0.01$) over the fire-constrained region, making the findings consistent with the approach employing the 12 years worth of MISR measurements.

RC: "Whether authors validated satellite and plume-rise model prior to this study?"

AC: Again, it seems that the reviewer did not carefully read the previous works of the author, in which careful validation of the measurements and models have already been performed. Perhaps, for clarity, additional paragraphs can be added to this work to further enhance this, without repeating verbatim. Specifically, a quick summary of the performance under the local conditions in Southeast Asia, which seems to be the reviewer's primary concern.

RC: "Why did authors use AOD and FRP from two different satellites instead a single satellite?"
AC: We did not. All of the AOD and FRP measurements used in the statistics and figures (except for figure 1) are from MODIS. We used MISR only to constrain in space and time the domain that was influenced by the fires "fire region" and no influenced by the fires "non-fire region". This is explained in detail in **sections 2.1 and 2.2**. The explanation includes the major rationale, since MISR cloud clears better over this region, but has a lower frequency of measurement.

RC: "How does the atmospheric stabilization due to direct effect of aerosols affect the vertical transport of aerosols?" and "This may be attributed to several other reasons"
AC: As mentioned in the article, there is an atmospheric stabilization due to both the DIRECT EFFECT and the SEMI-DIRECT EFFECT. There is literature to support this, some of which has been cited in the draft. It is an excellent question, and a question we are currently tackling. Additionally, we talk about the issue of localized convection also not being properly resolved. The fact of the matter is that, at the present time, there are hundreds of papers being published with regional models (i.e.: WRF-CHEM) and global models (i.e. GEOS-CHEM), which do not also address these issues at all. In fact, they are not even designed to allow for communication between the chemistry and the meteorology.

The rationale of this work was to follow their approach, which is a currently accepted approach in the community, and to do an extremely comprehensive study. There is currently no other paper that has analyzed more than 10,000 daily data points of CALIOP measurements, and run a model jointly with more than 3000 MODIS daily fire hotspots and meteorological measurements, over this region of the world, that we can find. In fact, the papers that are generally cited over this region of the world do not even mention what methodology they use to analyze the measured data, nor details of which versions of the data they are using. Frequently, they make mere comparisons with CALIOP or AOD image files, without carefully looking at the data and making sure it is of high quality. I have even seen such articles published in this prestigious journal.

RC: "This has nothing specific to about El Nino, general to all large-scale fire events."
AC: This is not true, and the reviewer knows this. While this was a large-scale fire event, it was very special. The Monsoon has generally arrived in October, and hence October is usually the transition from the burning season to the rain season. As such, the meteorology was completely different during this period of time. It was heavily influenced by El Nino. The length of the burning season, the wetness of the soil, the

large-scale meteorological flow, and such, were all not typical in this year. It is an interesting idea, however, to expand upon such and to compare the differences between El Nino and non El Nino years, however, the amount of data analysis to be required would be huge. In fact, this is a common mistake made by other authors in the past in this region of the world, and one of the major reasons why their results do not necessarily compare as well against measurements from AERONET, NOAA, Chinese measurement networks, etc.

RC: "Line 16: Authors mentioned that "our results are significantly different from what others are using". However, it is hard to find any discussion on this topic in later sections. Provide references to justify the statement."
AC: Thank you. While there are already some references, more will be added, and the discussion will be extended as well.

RC: "Line 39-46: Poor clarity and readability"
AC: This will be addressed. Thank you.

RC: "Line 58: hydroscopicity or hygroscopicity?"
AC: Hygroscopicity, thank you.

RC: "Line 101-107: Rewrite the sentence. Message is not clear."
AC: Thank you. This will be addressed.

RC: "Line 110: What is the "reasonable approximation" mentioned here?"
AC: References and some more detailed explanations of the physics will be added here. It is based on the physical relationship between backscatter and the aerosol optical properties, which are reasonably uniform when considered over the thousands of kilometers extent of the plume as a whole.

Changes to the Supplement

Formatted: Highlight

Supplement:

Detailed Methodology

The buoyancy flux parameter (F_B) **Equation A1** is a function of the temperature difference between the air (T_A) and the fire (T_F), the vertical motion of air (v) and the size of the fire, d (here always measured at 1km^2 in this work).

$$F_B = gv\frac{d^2}{4}\left(\frac{T_F - T_A}{T_A}\right) \quad \text{(A1)}$$

The buoyancy flux parameter has been found empirically to demonstrate whether the plume rise is buoyancy or momentum dominated. Under stable atmospheric conditions [Stone and Carlson, 1979], where the atmospheric lapse rate is ($L_A = \frac{\Delta T}{\Delta Z} < -5$), for a buoyancy dominated plume, (defined as where the difference between T_A and T_F is given in **Equation A2b1**), the plume rise height (Δh) is given by **Equation A2b2**, where (U) is the horizontal wind magnitude.

$$(T_F - T_A) > 0.01958 T_F \sqrt{v} \quad \text{(A2b1)}$$

$$\Delta h = 2.4\left(\frac{F_B}{.02U}\right)^{1/3} \quad \text{(A2b2)}$$

Whereas, for a momentum dominated plume (where the difference between T_A and T_F is less than the right hand side of **Equation A2b1)**, the height rise is given by **Equation A2b3**.

$$\Delta h = 1.5\left(\frac{\frac{V^2 d^2 T_A}{4\ T_F}}{\sqrt{.02}U}\right)^{1/3} \quad \text{(A2b3)}$$

On the other hand, under unstable atmospheric conditions (where $L_A > -5$), and where the plume rise is buoyancy dominated, the plume rise height is given by either **Equation A2b4** when $F_B > 55$ or **Equations A2b5, A2b6** when $F_B < 55$ [Woodward, 2010].

$$X^* = 14 F_B^{\frac{5}{8}} \quad \text{(A2b4)}$$

$$X^* = 34 F_B^{\frac{2}{5}} \quad \text{(A2b5)}$$

$$\Delta h = 1.6\frac{F_B^{\frac{1}{3}}(3.5X^*)^{\frac{2}{3}}}{U} \quad \text{(A2b6)}$$

Supplemental Figure 1: PDFs (x-axis is the height in km, and the y-axis is the probability distribution) of the monthly aggregated backscatter heights of the 10% [red] (top), 30% [dark blue], 50% [yellow], 70% [light blue], and 90% [black] levels. Note that there were no measurements on the 10th, 16th, and 20th.

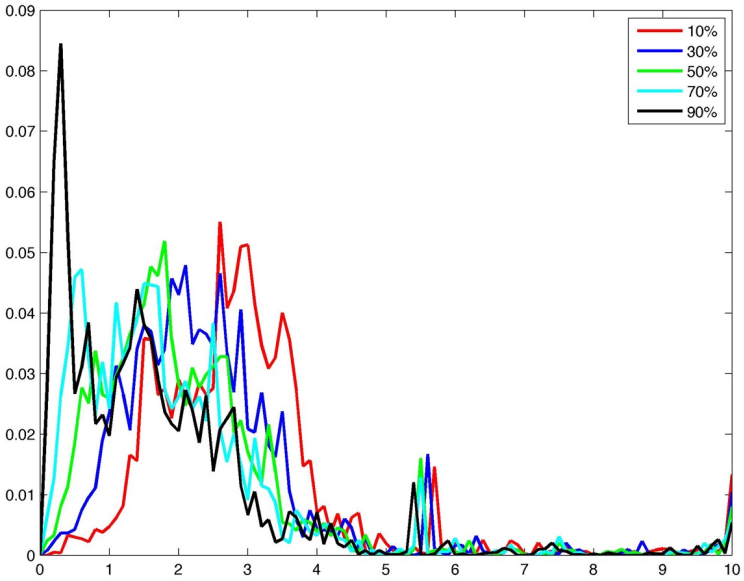

Supplemental Figure 2: Map of the monthly averaged MODIS AOD over the Maritime Continent. The day-to-day statistics are given in **Figure 3**. Regions in white have 0 valid AOD measurements throughout the entire time period, due to cloud cover.